Climate Dynamics (2005) 25: 19–36
DOI 10.1007/s00382-004-0491-0

**R. E. McDonald · D. G. Bleaken · D. R. Cresswell
V. D. Pope · C. A. Senior**

Tropical storms: representation and diagnosis in climate models and the impacts of climate change

Received: 20 August 2002 / Accepted: 22 October 2004 / Published online: 18 May 2005

Abstract Tropical storms are located and tracked in an experiment in which a high-resolution atmosphere only model is forced with observed sea surface temperatures (SSTs) and sea ice. The structure, geographic distribution and seasonal variability of the model tropical storms show some similarities with observations. The simulation of tropical storms is better in this high-resolution experiment than in a parallel standard resolution experiment. In an anomaly experiment, sea ice, SSTs and greenhouse-gas forcing are changed to mimic the changes that occur in a coupled model as greenhouse-gases are increased. There are more tropical storms in this experiment than in the control experiment in the Northeast Pacific and Indian Ocean basins and fewer in the North Atlantic, Northwest Pacific and Southwest Pacific region. The changes in the North Atlantic and Northwest Pacific can be linked to El Niño-like behaviour. A comparison of the tracking results with two empirically derived tropical storm genesis parameters is carried out. The tracking technique and a convective genesis parameter give similar results, both in the global distribution and in the changes in the individual basins. The convective genesis parameter is also applied to parallel coupled model experiments that have a lower horizontal resolution. The changes in the global distribution of tropical storms in the coupled model experiments are consistent with the changes seen at higher resolution. This indicates that the convective genesis parameter may still provide useful information about tropical storm changes in experiments carried out with models that cannot resolve tropical storms.

R. E. McDonald (✉) · D. G. Bleaken · D. R. Cresswell
V. D. Pope · C. A. Senior
Met Office Hadley Centre for Climate Prediction and Research, FitzRoy Road, Exeter, EX1 3PB, United Kingdom
E-mail: ruth.mcdonald@metoffice.gov.uk
Tel.: +44-1392-886947
Fax: +44-1392-885681

1 Introduction

Tropical storms are small-scale intense cyclonic systems that develop over the tropical oceans in regions of very warm surface water. They consist of an area of enhanced convection that has a horizontal scale of the order of hundreds of kilometres and the centre is warmer than the surrounding atmosphere. The cost of tropical storms both in terms of loss of life and economic cost can be devastatingly high and changes to tropical storms due to global warming may have large impacts on society.

Tropical storm-like features have been analysed in studies with numerical models that range from low-resolution climate general circulation models (GCMs), to regional climate models, to very high-resolution hurricane prediction models. The horizontal scale of tropical storms is much smaller than the horizontal grid-scale of most GCMs and because of this there has been some debate over the utility of GCMs in studying tropical storm behaviour (e.g. Lighthill et al. 1994; Henderson-Sellers et al. 1998). However, our analysis follows previous studies (e.g. Bengtsson et al. 1996; Sugi et al. 2002) in using a high-resolution global atmosphere only GCM.

Coupled atmosphere-ocean GCM experiments, run with increasing greenhouse gases, give enhanced sea surface temperatures (SSTs) and atmospheric moisture in the tropical region (Cubasch et al. 2001) that may change the intensity, location and variability of tropical storms (Henderson-Sellers et al. 1998). To date, the results of GCM experiments are inconclusive (see Giorgi et al. 2001). A low-resolution Met Office model gives more tropical disturbances (Haarsma et al. 1993), but higher resolution versions of the ECHAM3 and JMA models give fewer tropical storms (Bengtsson et al. 1996; Sugi et al. 2002), while other models give increases in the Northern Hemisphere and decreases in the Southern Hemisphere (Royer et al. 1998). Changes in intensity, diagnosed with regional models or hurricane prediction models, are more consistent (Giorgi et al. 2001), with most models producing more intense tropical storms (e.g. Knutson and Tuleya 1999; Walsh and Ryan 2000), although these changes are not all statistically significant (e.g. Walsh and Ryan 2000). An alternative technique for analysing tropical storm intensity is to use the theory of maximum potential intensity (MPI) of tropical storms (Emanuel 1987). Henderson-Sellers (1998) found an increase of 10–20% in the intensity of tropical storms under 2xCO_2 conditions using the MPI calculations of Holland (1997). Here we analyse changes in tropical storms in a global warming experiment carried out with a high-resolution model.

Two techniques for diagnosing tropical storms have been commonly used in global climate model experiments. The first technique locates and tracks individual cyclones, as centres of maximum relative vorticity which have a warm core (e.g. Haarsma et al. 1993; Bengtsson et al. 1995; Vitart et al. 1997). The second technique provides an estimate of tropical storm activity using a genesis parameter, which is calculated from seasonal means of the large-scale fields and so avoids the problems of simulating individual cyclones. We use both Gray's genesis parameter (Gray 1979; Watterson et al. 1995) and a convective genesis parameter (Royer et al. 1998). As in Walsh and Watterson (1997), we apply both the tracking technique and the two genesis parameters to data from experiments carried out with the high-resolution model. This allows us to diagnose the relative merits of the different analysis techniques. We also investigate if the tropical storm analysis techniques can provide information about tropical storm changes in experiments carried out with the lower resolution models that are typically used for coupled climate-change experiments.

We begin by describing our models, experiments, data and analysis techniques, and then we test how well tropical storms are represented in a present-day simulation carried out with the high-resolution model, in Sect. 3. In Sect. 4, we investigate how the frequency, intensity, and distribution of tropical storms change under global warming conditions in this model. Next, we examine the usefulness of the genesis parameters in diagnosing both present day and future tropical storms in the high-resolution model before using some of the components of these genesis parameters to explore the mechanisms of the changes and investigate if the changes are similar to those which occur during El Niño events. Finally, we test whether any useful information about tropical storms can be gained from experiments carried out with low-resolution models using either the tracking technique or the genesis parameters.

2 Models, experiments, data and analysis techniques

The model used for our experiments is based on the third generation Met Office coupled ocean-atmosphere model (HadCM3, Gordon et al. 2000), which is a version of the Met Office unified forecast and climate model (Cullen 1993). The atmosphere component of HadCM3 (HadAM3; Pope et al. 2000) has a horizontal resolution of 2.5° latitude by 3.75° longitude and 19 levels in the vertical. The ocean component has a horizontal resolution of 1.25° latitude by 1.25° longitude and 20 levels in the vertical. Experiment N48 has the same physics and horizontal resolution as HadAM3, but has 30 levels in the vertical. N48 is the horizontal resolution of the experiment, where N refers to the wave numbers around a latitude circle (see Pope and Stratton 2002 for details). Experiment N144 (Pope and Stratton 2002) is parallel to N48 but with an increased horizontal resolution of 0.83° latitude by 1.25° longitude. N48 and N144 were both run for 17 years and 3 months from 1/1/1979 to 1/3/1996 with observed SSTs and sea-ice boundary conditions applied as monthly means. HadAM3 is a different model to the Met Office model used by Haarsma et al. (1993) as the two models have different parameterizations of the physical processes. We use higher horizontal and vertical resolutions in N144 than in the experiments carried out by Haarsma et al. (1993). It is therefore likely that the results of our model will be different from those of Haarsma et al. (1993).

To investigate changes in tropical storms due to enhanced greenhouse gases, we run an anomaly experiment (WARM). This is parallel to N144, but the greenhouse-gas forcing, sea ice, and SST are changed so as to capture the changes that occur as greenhouse gases are increased in a HadCM3 coupled model experiment. The HadCM3 greenhouse gas experiment that we use is referred to as GHG and has historical increases in major and minor greenhouse gases from 1860 to 1990 and then increases as in scenario IS95a (Houghton et al. 1996) after 1990 (see Williams et al. 2001 for details). The greenhouse gas forcing in WARM is kept the same as in GHG and the sea-ice forcing fields are the individual monthly means from GHG for the period 2080–2100. We derive the SST forcing fields by adding the monthly mean differences between GHG and CON (the HadCM3 control experiment with pre-industrial greenhouse gases) to the observed monthly SST fields (as used in N144):

$$\mathrm{SST}(m,t) = \mathrm{SST}_O(m, 1979+t) + <\mathrm{SST}_\mathrm{G}(m) > - <\mathrm{SST}_\mathrm{C}(m)> + t * \frac{\mathrm{d}\overline{\mathrm{SST}_\mathrm{G}(m)}}{\mathrm{d}t} \quad (1)$$

where, $\mathrm{SST}_O\ (m,\ t)$ is the observed SST for month m and year $1979+t$; $<\mathrm{SST}_G\ (m)>$ is the 20-year mean (2080–2100) of GHG SST for month m; $<\mathrm{SST}_C\ (m)>$ is the 20-year mean of CON SST for month m; $\mathrm{d}\overline{\mathrm{SST}_\mathrm{G}(m)}\big/\mathrm{d}t$ is the rate of change of the global mean SST in GHG over the 20-year period; and t is the number of years from 2080 (not 2090, the centre of the averaging period). Experiment WARM begins on 1 December 2081 and runs for 17 years and 3 months. Averages are made over the final 15 years of the experiment. As the experiments are of relatively short length, we are going to look for the physical plausibility of any changes in tropical storms as greenhouse gases are increased as well as test the statistical significance of the results.

The tracking technique that we use to locate and track tropical storms is a two stage objective technique and is referred to as TRACKS (see Appendix). In the first stage (Hodges 1994), we track local centres of 850 hPa relative vorticity with a magnitude greater than 5×10^{-5} s^{-1}. In the second stage the tracks are filtered so that only those cyclones which develop over tropical ocean points between 30°S and 30°N and have a warm core are included in our analysis. We apply these criteria to remove mid-latitude systems. We refer to each system identified by TRACKS as a tropical storm (TS).

To validate our model tropical storms, we compare them to observed tropical storms (which we shall refer to as OBS) for the period 1 December 1978 to 1 December 1995. The data for the Southern Hemisphere, North Indian region and Northwest Pacific region are from the Joint Typhoon Warning Centre 'best track' datasets. The data for the North Atlantic (see Landsea 1993 and Jarvinen et al. 1984) is from the Tropical Prediction Centre 'best track' datasets and the data for the Northeast Pacific is from the Colorado State University/Tropical Prediction Centre 'best track' datasets (see Davis et al. 1984). The tracks of these observed tropical cyclones are determined in a manual post-analysis of all available observational data (e.g. see Landsea 1993 and Serrano 1997). We only include the tropical storms that attain a wind speed of at least 17 ms^{-1} at some point in their lifetime. The position of genesis of each observed track is defined as the first position of the track in the database. As the analysis technique is different to that used for our model data, it is possible that this may lead to differences between OBS and our model results. In an attempt to remove these differences, we apply our tracking technique to data from the European Centre for Medium Range Weather Forecasts (ECMWF) Re-Analysis datasets (ERA, Gibson et al. 1997; Kållberg 1998). We use data for the period December 1978 to February 1994 with a resolution of 1.0° latitude × 1.0° longitude. However, there are far fewer TSs in ERA (not shown) than in either OBS or N144 (see Sect 3). Walsh (1997) found a similar result and concluded that the TSs were poorly analysed in the ERA data. Therefore, we do not present TRACKS results from the ERA data in this study.

The empirical methods that we use to diagnose tropical storm genesis are Gray's genesis parameter (GrayGP: Gray 1979; Watterson et al. 1995) and Royer's convective genesis parameter (ConvGP: Royer et al. 1998). The GrayGP (see Eq.1 of Watterson et al. (1995)) is the product of a dynamical potential, that is derived from: the Coriolis effect, the magnitude of the cyclonic relative vorticity and wind shear; and a thermal potential, that is derived from: ocean heat content, moist static stability and relative humidity. The ConvGP uses a measure of convective activity in place of the thermal potential of the GrayGP. We calculate the ConvGP by applying a constant proportionality factor (k) to the total convective precipitation. We use the same value of k (0.1159) for N144 and WARM and this is chosen so that the N144 ConvGP global mean annual total of cyclogenesis is the same as that in the GrayGP. Seasonal mean fields are used to calculate the genesis parameters for each season and the four seasonal fields are added to give an annual total of tropical storm genesis. We calculate both diagnostics over the region 35°S to 35°N as this is where the majority of tropical storms form.

3 How well does the high-resolution model simulate tropical storms?

We compare the structure of a single model tropical storm to an example of an observed typhoon (from Gray 1979) in Fig. 1. In this example the model captures both the strong cyclonic flow and the in-flow at low levels, but both maxima are located too far from the centre of the storm (compare Fig. 1a, c and b, d). At the upper levels the radial outflow appears too strong, too low and confined near to the storms (Fig. 1b, d) and the anticyclonic flow begins too far from the centre of the storm (Fig. 1a, c). This single example illustrates that the N144

Table 1 Annual mean and standard deviation (in parenthesis) of number of tropical storms per season in each ocean region for OBS, N144 and differences of N144 minus OBS

	Tropics 30°S–30°N	Northern Hemisphere 0–30°N	Southern Hemisphere 0–30°S	North Indian	Northwest Pacific	Northeast Pacific	North Atlantic	Southwest Indian	Southwest Pacific
OBS	82 (9.7)	58 (6.9)	25 (4.9)	4 (2.1)	26 (3.1)	19 (5.2)	8 (3.2)	11 (2.5)	14 (4.2)
N144	144 (12.1)	71 (10.9)	74 (7.1)	12 (3.1)	40 (12.7)	10 (5.0)	8 (2.8)	22 (4.7)	47 (5.3)
Difference N144-OBS	**61.2**	**13.4**	**48.8**	**7.4**	**14.1**	**−8.9**	0.4	**11.5**	**32.8**
Correlation of the number of tropical storms in each season for OBS and N144	0.36	0.46	0.13	0.16	0.53	−0.02	0.34	−0.29	0.26

Differences that are statistically significant at the 95% confidence level, using a two-sided equal variance Student's t test, are shown in bold. Also shown are the correlations of the number of tropical storms in each season for OBS and N144. Absolute correlations greater than 0.54 (0.56) are significant at the 5% level using a two-sided test for the Northern Hemisphere (for the Southern Hemisphere). The season is from January to December in the Northern Hemisphere and from July to June (of the following year) for the Southern Hemisphere, giving 17 years of data in the Northern Hemisphere and 16 years of data in the Southern Hemisphere. The N144 tropical storms are TSs as diagnosed using TRACKS and the ocean basins are defined on Fig. 2

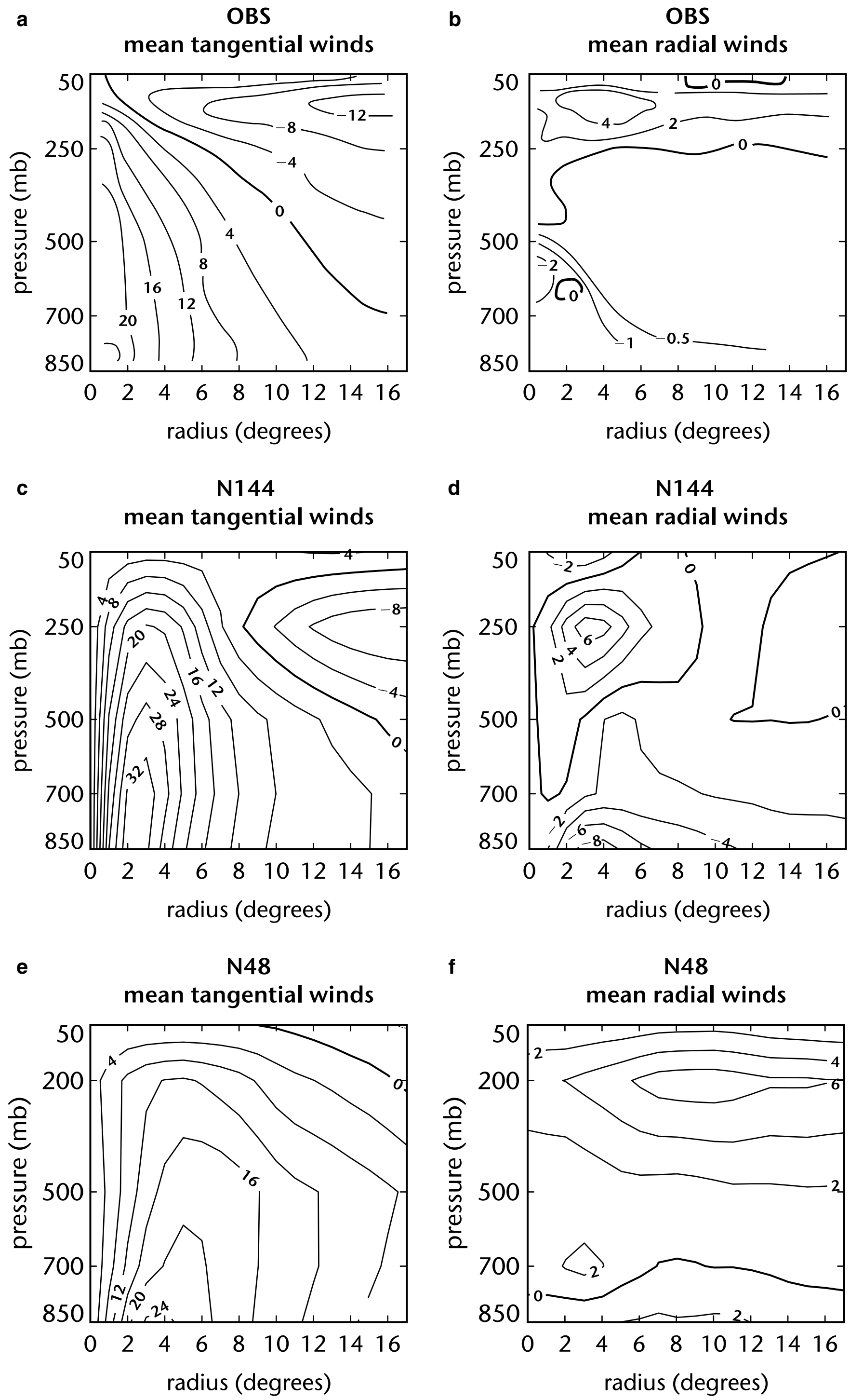

Fig. 1 Two-dimensional cross section of wind for a mean observed typhoon wind structure (adapted from Gray (1979)), for one of the strongest tropical storms from the N144 experiment (located in the SW Pacific to the North of Australia) and for one of the strongest tropical storms from the N48 experiment (located in the Northwest Pacific near to Japan). **a** Observed tangential winds for a mean typhoon (from Gray (1979)), **b** observed radial winds for a mean typhoon (from Gray (1979)), **c** N144 mean tangential winds, **d** N144 mean radial winds, **e** N48 mean tangential winds, and **f** N48 mean radial winds. The contour interval in **a**, **c** and **e** is 4 ms^{-1} and the contour interval in **b**, **d** and **f** is 2 ms^{-1}

model is capable of simulating the large-scale features of TS without capturing the detail or the intensity of the inner cores, which are typically smaller than the horizontal grid-scale of N144 and so cannot be explicitly resolved.

We now compare TS genesis in N144 to that of the observed (OBS) tropical storms (Table 1 and Fig. 2). In general, TS genesis occurs in the same regions in N144 as in OBS, with the exception of the South Atlantic, where TS genesis occurs in N144 but is rarely observed (Fig. 2). A tropical storm-like cyclone was observed in March 2004 off the coast of Brazil, in the region where this model produces tropical storms. The number of TSs simulated in N144 is significantly different from the number of observed tropical storms in all but the North Atlantic basin (Table 1). N144 has approximately the same numbers of TSs in the Southern Hemisphere as in the Northern Hemisphere, whereas OBS has fewer in the Southern Hemisphere than in the Northern Hemisphere. This is a common feature of tropical storms in climate models (e.g. Sugi et al. 2002) and it is possible that data sparseness in the Southern Hemisphere is affecting the observed numbers here. The Northeast Pacific basin is the only region that simulates fewer tropical storms than there are in OBS (Table 1). This may be because tropical storms in this region are more difficult to model due to their modest size (Serrano 1997). The lifetimes of the model tropical storms are too short in all basins (Fig. 3) and the reasons for this are not clear. It may be due to the different analysis techniques between OBS and TRACKS, but it is also possible that TRACKS is splitting individual tracks into 2 shorter tracks and hence increasing the number of storms formed, which would be consistent with the overestimate of the total number. Most of the tropical storms occur at the correct time of year (Fig. 4), with the exception of the summer months in the North Indian basin (Fig. 4a), but the numbers of TSs in each month are significantly different from OBS in the majority of the peak season months in all basins (Fig. 4). The errors in timing in the North Indian basin may be due to TRACKS classifying the model's monsoon depressions, which develop in the Bay of Bengal during the summer monsoon season, as TSs and so giving high counts between May and October.

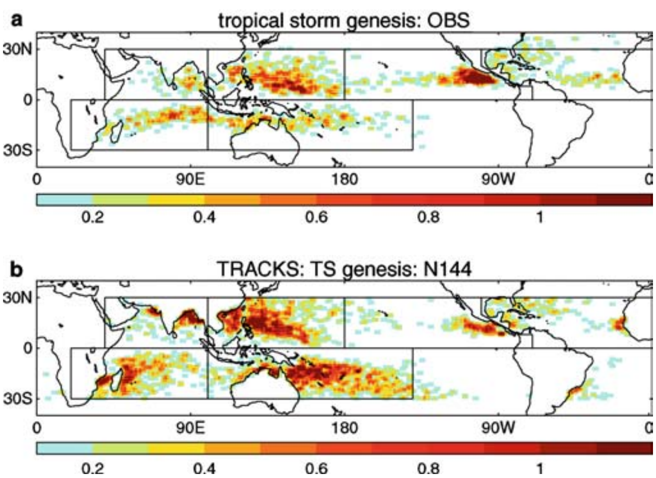

Fig. 2 Density of tropical storm genesis for: **a** OBS (17 years, 1 December 1978 to 1 December 1995) and **b** N144 (17 years, 1 December 1978 to 1 December 1995). For OBS the genesis point is the first point in the 'best track' data and to be included in our analysis an observed tropical storm must attain a wind speed of 17 ms^{-1} at some point during its life. For N144 the TSs are diagnosed using TRACKS and the point at which cyclogenesis occurs is defined as the grid point where the magnitude of the relative vorticity at the centre becomes at least $5.0\times10^{-5}\ s^{-1}$. The fields have been 9-point area averaged. The shading interval is 0.1 tropical storms per 0.83° latitude×1.25° longitude area per 17 year. The region of each ocean basin is also shown and the basins are defined as: North Indian (40°E–100°E, 0°–30°N); Northwest Pacific (100°E–180°, 0°–30°N); Northeast Pacific (180°–70°W, 0°–30°N, but not including any part of the North Atlantic); North Atlantic (100°W–0°, 0°–30°N, but not including any part of the Northeast Pacific); Southwest Indian (20°E–100°E, 0°–30°S) and Southwest Pacific (100°E–140°W, 0–30°S)

The standard deviations in Table 1 show that N144 has a greater variability than OBS in all but the Northeast Pacific and North Atlantic basin. To give an indication of N144's ability to simulate realistically the inter-annual variability of TSs frequency from the SST variability, we correlate (as in Vitart et al. 1997) the seasonal mean number of TSs in N144 with the number in OBS for each basin (Table 1). None of the correlations are significant and this suggests that either processes, other than the direct SST effect, are controlling the variability of tropical storms, or that the model is not realistically simulating the effects of SSTs on TS activity.

We now consider some of the links between errors in the large-scale circulation and in the simulation of tropical storms. The locations of observed tropical storm genesis show a strong association with regions of climatological minimum or zero vertical wind shear between the lower and upper troposphere (Gray 1968, 1979). The vertical wind shear of the horizontal wind (Fig. 5a, b) is weaker in N144 than in ERA to the south of the Southern Hemisphere regions where there are too many TSs in N144 (Fig. 2). However in other regions (e.g. Northwest Pacific and North Indian basins) the wind shears are too strong in N144 and there are still too many TSs.

The amount of tropical convective precipitation is also strongly linked to the number and intensity of tropical storms and in turn the presence of convective precipitation is favourable for cyclogenesis. Here we compare our model to seasonal mean precipitation data from the Climate Prediction Centre (CPC) Merged Analysis of Precipitation (CMAP) dataset (Xie and Arkin 1997), for the period 1979–1988 (Fig. 5c). N144 shows many differences to observations in total precipitation and these correspond closely to the differences seen in TS genesis (compare Figs. 2 and Fig. 5c).

In general the mean spatial and temporal distributions of tropical storms in N144 are good, even though the model resolution is larger than the scale of the intense core of observed tropical storms. This gives us some confidence that the physical mechanisms that form the model tropical storms are realistic. The errors in the simulation of the large-scale atmosphere flow and convective precipitation are consistent with some of the errors in the simulation of the numbers of tropical storms. A more detailed study of the model's genesis process is required to unravel the mechanisms of the errors completely. However, these results are consistent with those of other authors who have shown that models can resolve tropical storm-like disturbances without simulating the details of the central core (e.g. Bengtsson et al. 1995; Vitart et al. 1997), suggesting that models can be useful tools for understanding the response of tropical storms to climate change.

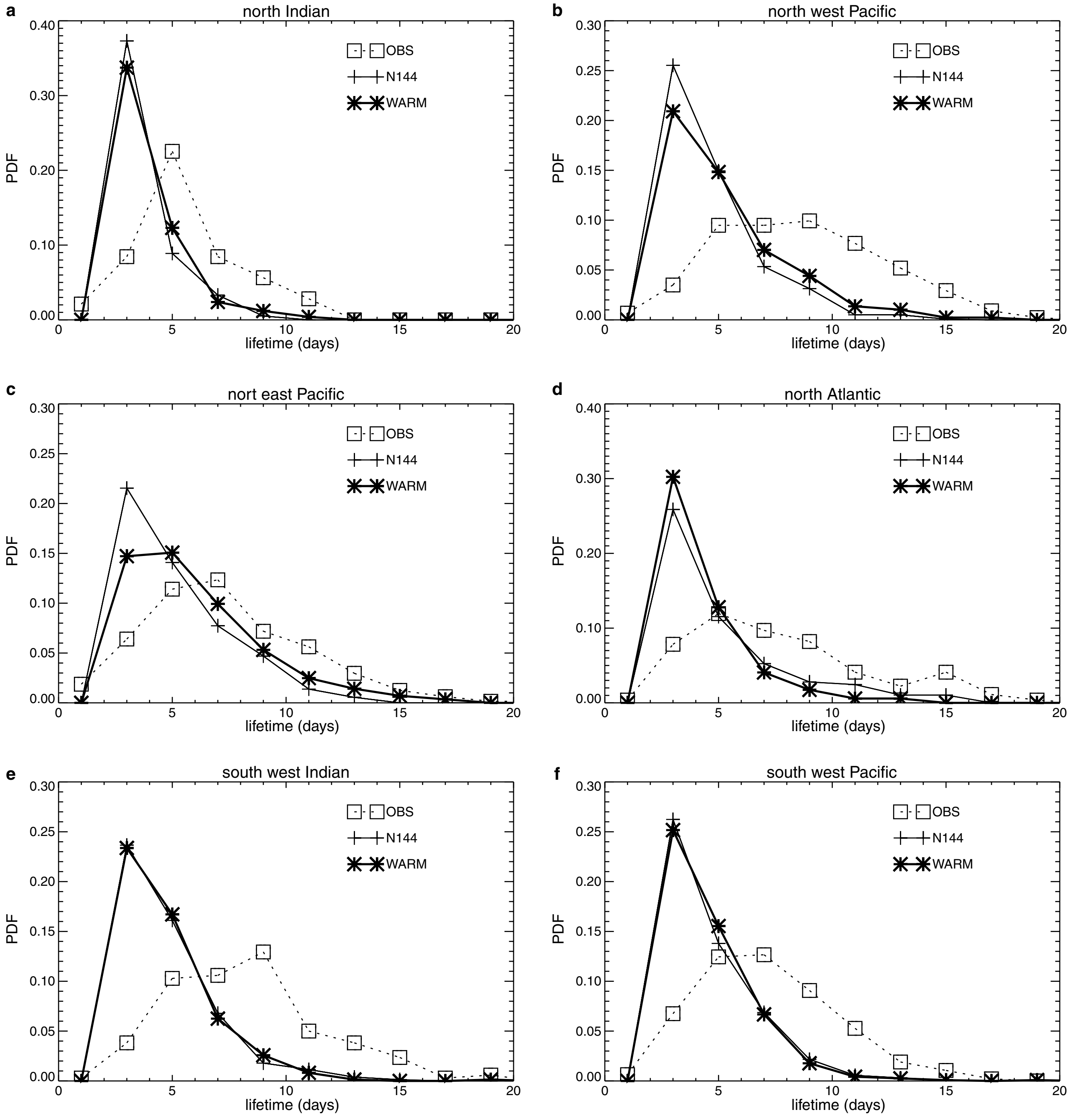

Fig. 3 Probability density function (PDF) of the lifetime of tropical storms in OBS (17-year mean, *squares and dotted lines*) and TSs as diagnosed by TRACKS for N144 (17-year mean, *plus and thin solid lines*) and WARM (15-year mean, *asterisk and bold solid lines*). The observations are for tropical cyclones with a maximum wind >17 ms^{-1}. **a** North Indian, **b** Northwest Pacific, **c** Northeast Pacific, **d** North Atlantic, **e** Southwest Indian and **f** Southwest Pacific. We define the lifetime, in days, of a model TS as the number of 12 hourly positions divided by 2 and the lifetime of a tropical storm in OBS as the number of 6 hourly positions divided by 4, except in the Northwest Pacific basin, where the 6 hourly positions where unavailable, so the lifetimes for this basin are taken directly from the "best track" data

4 What are the changes in tropical storms under global warming conditions?

In this section we compare the tropical storms simulated under the climate change conditions of experiment WARM to those simulated in present day conditions by N144. There are fewer TSs in WARM than in N144 in both hemispheres (Table 2), the 3% decrease in the Northern Hemisphere is not significant but the 10% decrease in the Southern Hemisphere is

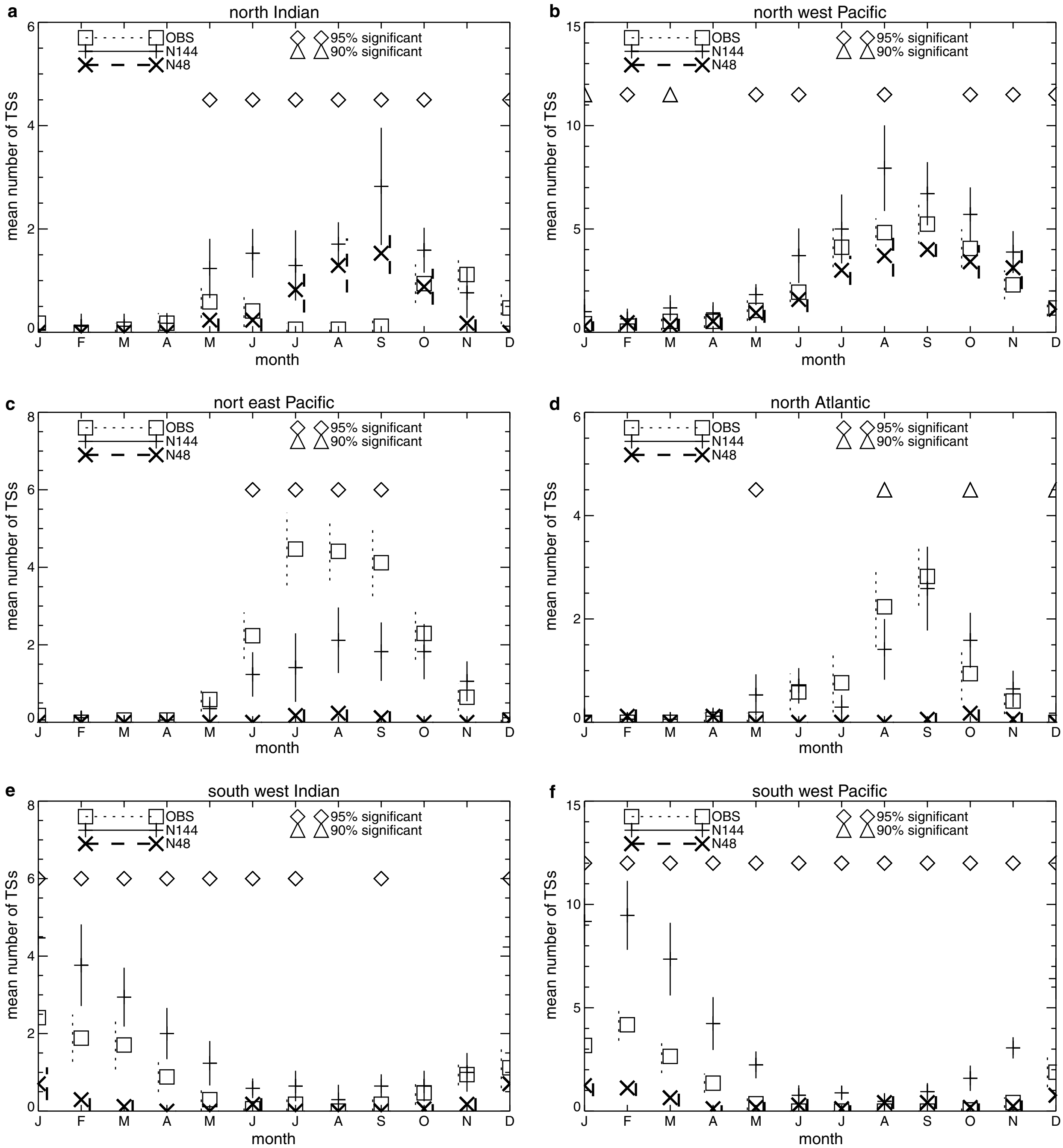

Fig. 4 Mean number of tropical storms per month and standard deviation (vertical lines) for OBS (17-year mean, *squares and dotted lines*) and TSs as diagnosed by TRACKS for N144 (17-year mean, *plus and thin solid lines*) and N48 (17-year mean, *multi and bold dashed lines*). The observations are for tropical cyclones with a maximum wind > 17 ms^{-1}. **a** North Indian, **b** Northwest Pacific, **c** Northeast Pacific, **d** North Atlantic, **e** Southwest Indian and **f** Southwest Pacific. We use a two-sided Student's *t* test to test the significance of the differences between N144 and OBS. The differences that are significant at either the 95 or 90% level are indicated by *diamonds* (95%) and *triangles* (90%) above the results for each month

significant. The 6% global decrease in TSs is consistent with the results of Bengtsson et al. (1996) and Sugi et al. (2002).

The most noticeable difference between WARM and N144 is the extended region of genesis in the Northeast Pacific (Fig. 6b and compare Fig. 2b to Fig. 6a). Overall the change in WARM shows a complex pattern of response with no consistent sign of change (Fig. 6b). In the Northwest Pacific TS genesis occurs further east than in N144. This is similar to the observed response to El Niño conditions (e.g. Wu and Lau 1992) and we explore the relationships between tropical storms and the phase of ENSO (El Niño—Southern Oscillation) in Sect. 6. There are significant increases in the North Indian and Northeast Pacific basins and significant decreases in the Northwest Pacific, North Atlantic and Southwest Pacific

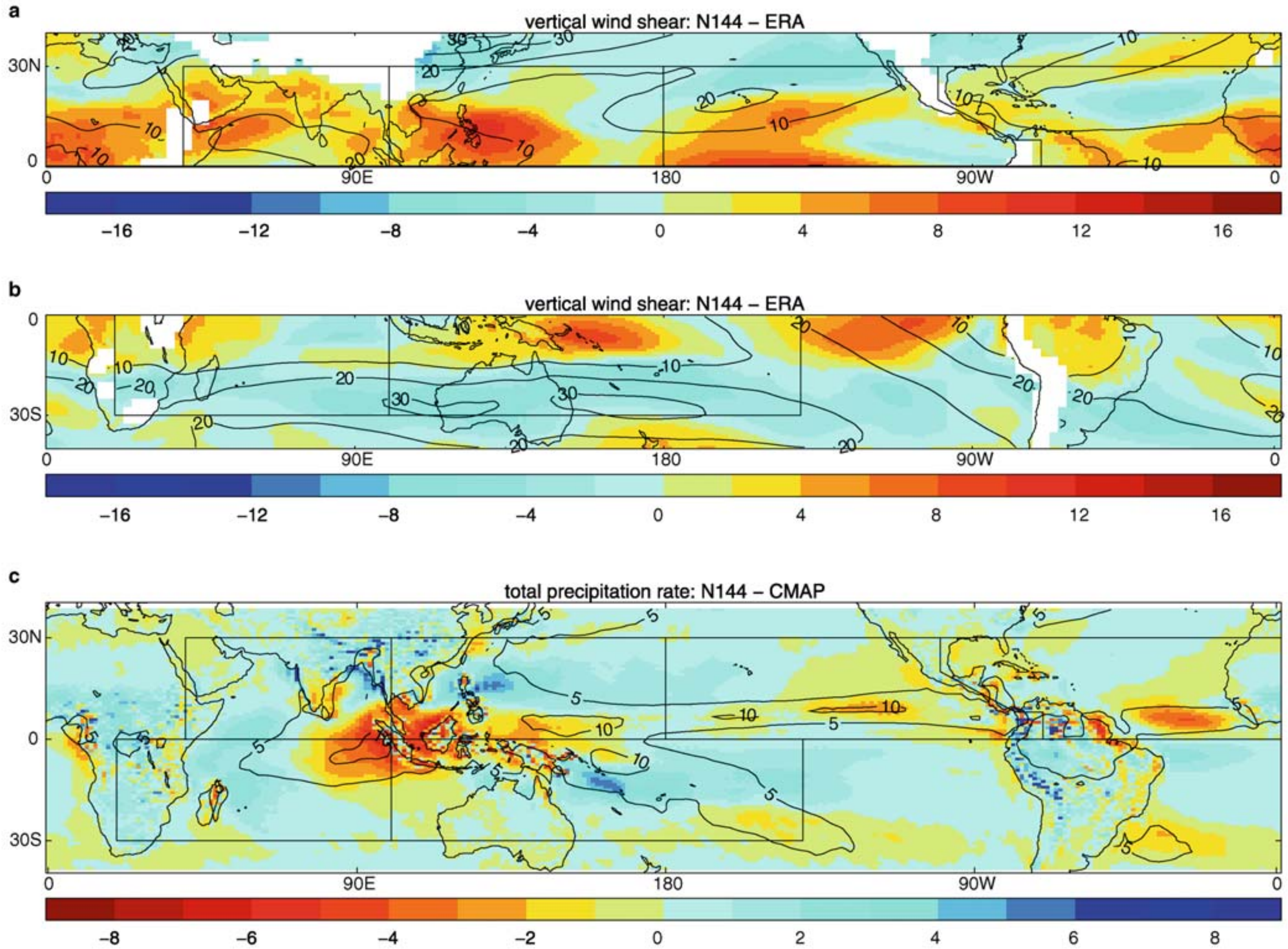

Fig. 5 Mean vertical shear of horizontal wind for N144 (17-year mean) minus ERA (1979–1995). The averages are over June to November for the Northern Hemisphere (**a**) and December to March for the Southern Hemisphere (**b**). Vertical shear is defined as the magnitude of the difference vector between the 200 and 850 hPa horizontal wind vectors. The shading interval is 2 ms^{-1} per 650 hPa. ERA is also shown, as contours, at 10, 20 and 30 ms^{-1} per 650 hPa. **c** Annual mean total precipitation rate for N144 (10-year mean) minus CMAP (1979–1988) with a shading interval of 1 mm day^{-1}. The colour table has been reversed in **c** so increases in precipitation are shown in *blue*. CMAP is also shown, as contours, at 5 and 10 mm day^{-1}

basins (Table 2). The increases in the North Indian and Northeast Pacific basins occur in the peak season and are significant (Fig. 7a, c). In the North Indian basin the simulation of too many TSs by N144 between May and October is enhanced in WARM compared to N144 (Fig. 7a). The decreases in TSs occur during August to October in the Northwest Pacific (Fig. 7b) and from December to March in the Southwest Pacific (Fig. 7f). The decrease in the North Atlantic is significant during July and September (Fig. 7d) and the increase in the Southwest Indian basin is significant during April (Fig. 7e). There is some evidence of longer lifetimes in the Northwest Pacific and Northeast Pacific regions and of shorter lifetimes in the North Atlantic region (Fig. 3). However, none of these changes in lifetimes are significant.

It is important to look at any changes in the intensity of the tropical storms. In this study we use the maximum value of the 850 hPa relative vorticity at the TS centres along each TS track to give an estimate of the maximum intensity of each TS. We use relative vorticity rather than surface wind as 12-hourly surface wind data was not available in these experiments. Although there are less TSs in WARM over the tropics, there is a shift in the intensity distribution to more intense TSs (Fig. 8), with some significant decreases in the number of weaker systems and some significant increases in the number of more intense systems.

We will investigate the mechanisms of the changes in tropical storms in Sect. 6, but first we will investigate the use of the genesis parameter for diagnosing tropical storm genesis.

Table 2 Annual mean and standard deviation (in parenthesis) of number of tropical storms per season in each ocean basin for WARM (15-year mean) and the differences and percentage changes of WARM minus N144

	Tropics 30°S–30°N	Northern Hemisphere 0–30°N	Southern Hemisphere 0–30°S	North Indian	Northwest Pacific	Northeast Pacific	North Atlantic	Southwest Indian	Southwest Pacific
WARM	135 (6.7)	69 (8.5)	67 (9.5)	17 (4.8)	28 (8.8)	18 (7.2)	6 (2.6)	24 (4.4)	39 (6.8)
WARM-N144	**−9.2**	−2.3	**−7.0**	**5.1**	**−12.2**	**8.0**	**−2.6**	2.1	**−8.3**
%change (%)	6	3	10	45	30	78	32	10	18

Differences that are statistically significant at the 95% confidence level, using a two-sided equal variance Student's *t* test, are shown in bold. The season is from January to December in the Northern Hemisphere and from July to June (of the following year) for the Southern Hemisphere. The N144 and WARM tropical storms are TSs as diagnosed using TRACKS

5 Do the genesis parameters give similar distributions of tropical storms to TRACKS?

Here, we test the use of two tropical storm genesis parameters (Ryan et al. 1992; Watterson et al. 1995; Royer et al. 1998). The pattern and magnitude of cyclogenesis in the GrayGP and ConvGP are broadly similar to those in TRACKS (compare Figs. 9a, b to 2b) but there are some notable differences in both the positions and magnitude of the maximum genesis regions. The annual mean number of tropical storms for the N144 ConvGP (Table 3) is 86 in the tropics, which is very similar to the observed number of 82, but there are too few tropical storms in the Northern Hemisphere and too many in the Southern Hemisphere. This result is the same as we found with TRACKS and was also found by Watterson et al. (1995). The annual mean GrayGP results for the tropics, Northern Hemisphere and Southern Hemisphere are the same as for the ConvGP and are not shown. As with the TRACKS results the correlations between OBS and N144 ConvGP are not significant.

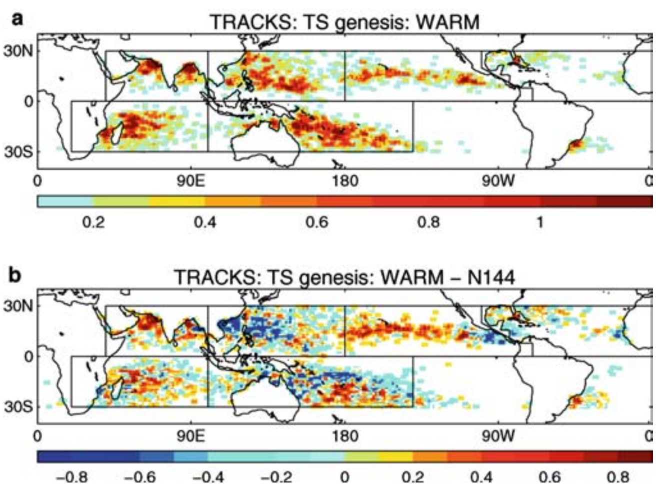

Fig. 6 Density of TS genesis as diagnosed by TRACKS for **a** WARM (15 years, 1 December 2082 to 1 December 2097) and **b** WARM (15 years) minus N144 (15 years, 1 December 1979 to 1 December 1994). The fields have been nine point area averaged. The shading interval is 0.1 TS per 0.83° latitude×1.25° longitude area per 17 year. For consistency with WARM only 15 year of N144 are used

(Table 3). The annual cycles of TS genesis in each basin from the GrayGP and the ConvGP techniques are similar to both the observed annual cycles and those produced when using TRACKS, although they differ in magnitude (Table 4 for Northeast Pacific and North Atlantic).

The GrayGP increases everywhere in WARM compared to N144 (not shown). As the GrayGP relies on SST relative to 26°C to limit the domain in the present day climate and Gray (1979) considered that heat energy from the ocean was relevant, it is possible that a higher SST threshold could be successfully used for the warmer climate. However we have not tried this in our study and have instead followed the method described in Royer et al. (1998) and used the ConvGP for the WARM experiment. Therefore, here we show only the pattern of changes in the ConvGP (Fig. 9c). These changes are similar to the changes in TS genesis (as defined by TRACKS) in WARM (Fig. 6b) in most regions. However the annual mean changes for the tropics and Northern Hemisphere are of opposite sign to those in TRACKS and there is no change in the Southern Hemisphere (compare Tables 2 to 3). The different response of the GrayGP compared to TRACKS and the ConvGP can also be seen in the annual cycles for the North Atlantic and Northeast Pacific basins (Table 4). Similar results are obtained for all basins, but we have chosen these two basins to illustrate the differences in the responses of the two genesis parameters. The ConvGP response in WARM is qualitatively similar to that of TRACKS in all basins (Table 4). The comparison is better for the individual basins than for the larger regions in Table 3. In contrast the GrayGP increases throughout the year in every basin (Table 4). In the Northeast Pacific the shift in the maximum tropical storm activity from JJA to SON, which occurs in TRACKS, also occurs in the ConvGP but does not occur in the GrayGP. In the North Atlantic the peak season is earlier than in TRACKS in both the GrayGP and the ConvGP and this difference occurs in both N144 and WARM.

In general, our results support the conclusions of Ryan et al. (1992) and Royer et al. (1998) that the GrayGP is dominated by the changes in the SSTs under global warming conditions. Therefore, although both the GrayGP and the ConvGP diagnose tropical storm

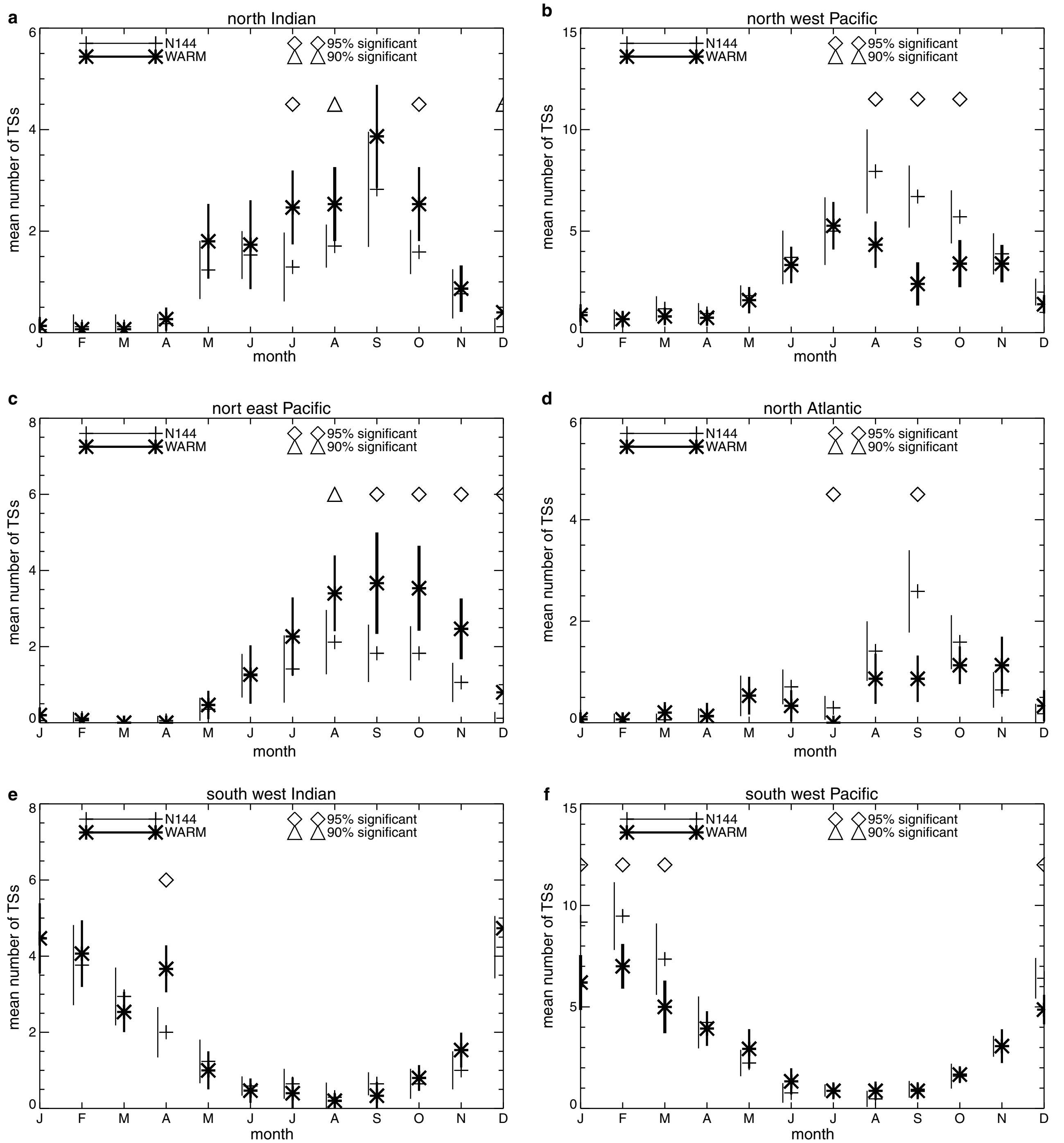

Fig. 7 Mean number of TSs per month and standard deviation (*vertical lines*) as diagnosed by TRACKS for N144 (17-year mean, *plus and thin solid lines*) and WARM (15-year mean, *asterisk and bold solid lines*). **a** North Indian, **b** Northwest Pacific, **c** Northeast Pacific, **d** North Atlantic, **e** Southwest Indian and **f** Southwest Pacific. We use a two-sided Student's *t* test to test the significance of the differences between WARM and N144. The differences that are significant at either the 95 or 90% level are indicated by *diamonds* (95%) and *triangles* (90%) above the results for each month

genesis well in the present day N144 simulation, the GrayGP is not as useful as the ConvGP for diagnosing changes in tropical storms.

6 What are the mechanisms of the changes in tropical storms?

To explain the differences in tropical storms in WARM compared to N144 we look at changes in some of the large-scale fields that are components of the genesis parameters. We begin with the SSTs, which contribute to the thermal potential of the GrayGP. One of the mean conditions which is favourable for tropical storm genesis is an SST above 26.5°C (Palmen 1948), so an increase in SSTs is likely to have an impact on tropical storms. It is often thought that an increase in the area with SSTs above 26.5°C leads to an increase in the region of tropical cyclogenesis; however, this has been shown by others (e.g. Henderson-Sellers et al. 1998) not to be the case. A comparison of the SST changes (Fig. 10a) with the TS genesis changes (Fig. 6b) shows that the changes in our model are consistent with this conclusion. The increases in TS genesis in the central North Pacific are where the SST warming has shifted the 26.5°C isotherm north, making the SSTs in this region above 26.5°C in WARM but not in N144. However, in other regions (e.g. North Atlantic and Northwest Pacific) the SSTs have increased and there are fewer TSs. Therefore the SST changes do not explain all of the changes in TSs. Hence the GrayGP does not give the same changes in tropical storms as TRACKS. The thermal potential part of the GrayGP over-responds as it is dominated by the SST changes.

We now investigate the dynamical components of the mechanisms of the changes in tropical storms. Gray (1979) found that tropical storms form in regions where there is cyclonic and convergent flow at lower levels, divergent flow at upper levels and low levels of vertical wind shear. Therefore, we consider the relative vorticity on 850 hPa and the vertical wind shear, which are both components of the dynamical potential and the velocity potential on 850 h Pa. The 850 hPa flow (Fig. 10b) is more anti-cyclonic and divergent where there are fewer TSs, and more cyclonic and convergent where there are more TSs. We showed in Sect. 3, how low vertical wind shear gave high values of tropical storm genesis in N144. The opposite mechanism occurs in the region around Central America, as there is an increase in the vertical

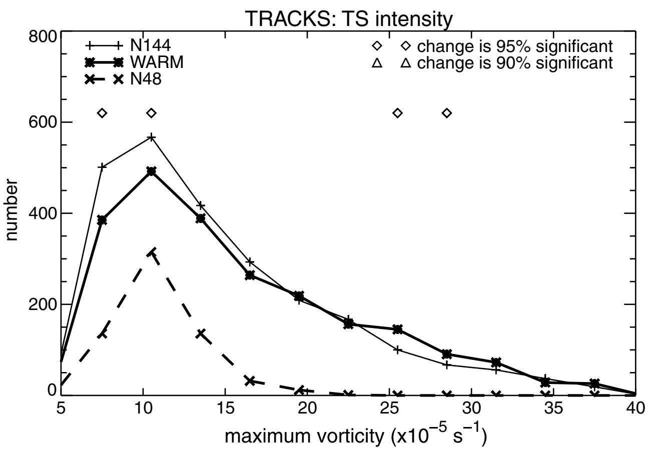

Fig. 8 Frequency distribution of the maximum magnitude of relative vorticity at the TS centre for all TSs in N144 (17 years, *plus and thin solid lines*), WARM (15 years scaled to 17 years, *asterisk and bold solid line*), and N48 (17 years, 1 December 1978 to 1 December 1995 *multi and bold dashed lines*). The units of magnitude of relative vorticity are 10^{-5} s^{-1}. We use a 2-sided Student's t test to test the significance of the differences between WARM and N144. The differences that are significant at either the 95 or 90% level are indicated by *diamonds* (95%) and *triangles* (90%) above the results

shear of the horizontal wind (Fig. 10c) and fewer TSs (Fig. 6b).

Finally, we consider the convective rainfall (Fig. 10d), as this is the basis for the convective potential and we showed that this is also linked to tropical storm genesis in N144 in Sect. 3. The changes in rainfall are connected with the changes in TSs in some regions. For example, there is increased rainfall in regions where there are more TSs (e.g. North India and central North Pacific) and less rainfall where there are fewer TSs (e.g. Northwest Pacific). However, the changes are not as well linked in the Southern Hemisphere, particularly near 10°S (in both the Southwest Indian basin and near Australia) where the rainfall increases and the number of tropical storms decreases. The changes correspond better in the central South Pacific where the southward shift in TSs in the Southwest Pacific can also be seen in the rainfall. The increases in the number of TSs will, in turn, give increased convective rainfall. The changes in SSTs may be driving the changes in TSs through an indirect effect via the changes in rainfall.

The changes in the SSTs between N144 and WARM (Fig. 10a) are similar to the pattern of warming that occurs during an El Niño event in the tropical Pacific (e.g. Philander 1990). Several studies have found that ENSO has strong physical links with tropical storm numbers in the North Atlantic and Northwest Pacific (e.g. Gray 1984). Therefore, we now explore the similarity between the changes in tropical storms in WARM and the changes in tropical storms which occur due to ENSO. To categorise years as either El Niño or La Niña, we use the SSTs in the NINO3 region (5°N to 5°S, 150° to 90°W). We first calculated the 15-year NINO3 area mean for each season. We then calculate the individual seasonal means over the NINO3 region. If an individual seasonal mean SST is greater than 0.5 K above the 15-year seasonal average then that season is classed as El Niño. If a seasonal mean SST is more than 0.5 K below the 15-year seasonal average then that season is classed as La Niña. The remaining seasons are classed as neutral. A year in which two or more consecutive seasons are classed as El Niño seasons is classed as an El Niño year and a year in which two or more consecutive seasons are classed as La Niña seasons is classed as a La Niña year. Other years are classed as either neutral or transitional, if they switch between El Niño and La Niña. The ConvGP El Niño and La Niña composites (Fig. 11) are then made from the means over the El Niño years and the La Niña years, respectively. The samples of years counted as El Niños (6 years) or La Niñas (4 years) in our study are likely to be too small for any significance to be given to these results; however, we show later that similar results are obtained with 100 years of data from HadCM3 CON.

The differences between the ConvGP El Niño and La Niña composites for N144 (Fig. 11) shows some similarities to the change in the ConvGP from N144 to WARM (Fig. 9c) in the North Atlantic, Northeast Pacific and Northwest Pacific. The North Pacific and

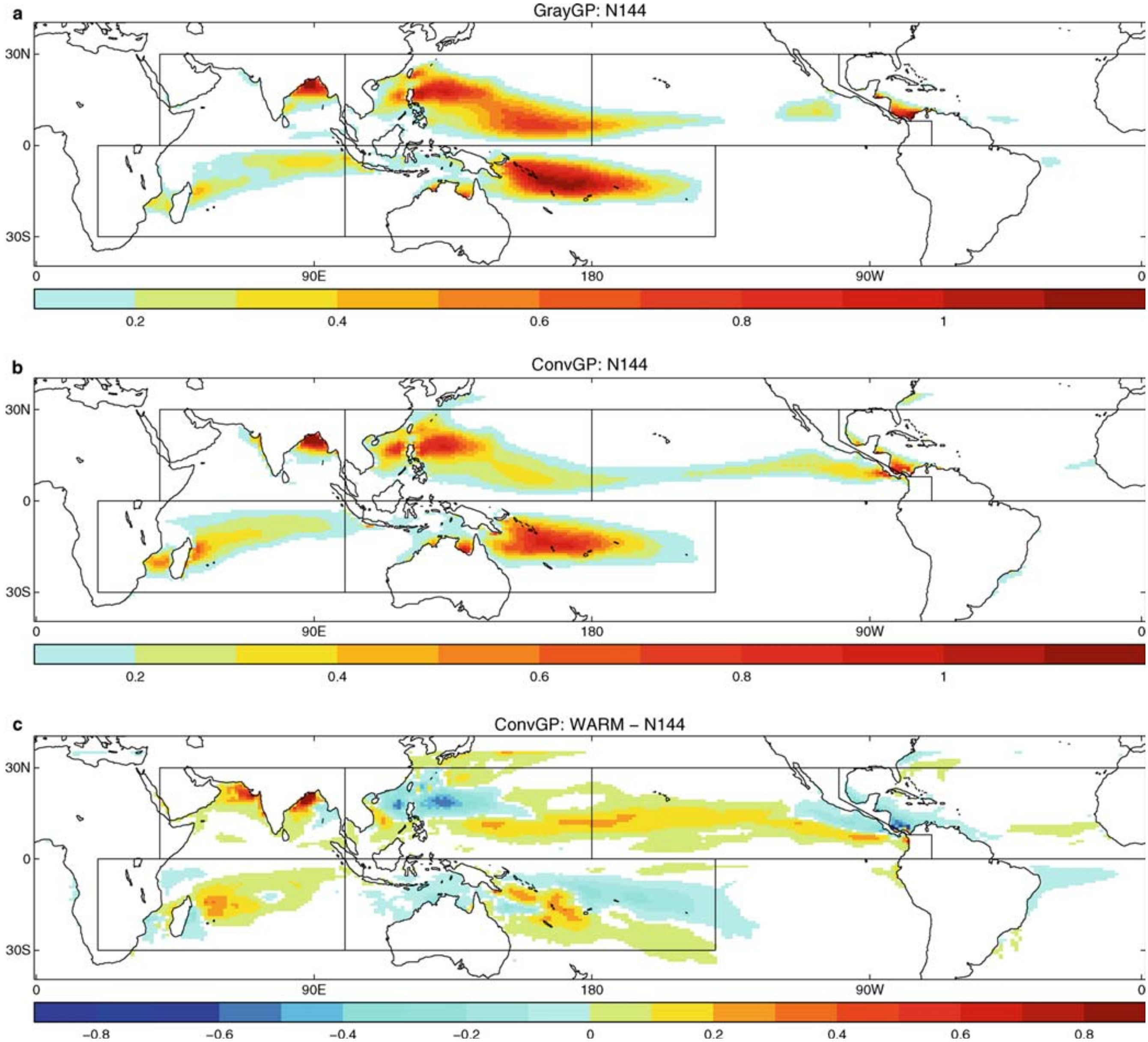

Fig. 9 Density of tropical storm genesis for N144 (17-year mean) as defined by **a** GrayGP and **b** ConvGP. **c** Tropical storm genesis as diagnosed by the ConvGP for WARM (15-year mean) minus N144 (17-year mean). The shading interval is 0.1 tropical storms per 1° latitude×1° longitude area per 17 year

North Atlantic regions are where the pattern of SST response in WARM (Fig. 10a) is most like the observed response to ENSO. In the Southwest Pacific the change in the ConvGP in WARM is opposite to the change which occurs in N144 due to ENSO. This is because the change in SST gradient in WARM across the South Pacific (Fig. 10a) is opposite to the ENSO related change in SST gradient. We repeat the ENSO analysis with TSs from TRACKS, but the short length of our experiments means that there are only a few TSs in each of the composites. The sample sizes are therefore too small for any signal to be apparent and hence, we do not show the results here.

The mechanisms that cause the changes in tropical storms during El Niño are occurring in WARM. For example, during El Niño events the anomalous warming in the east Pacific gives increased upper level westerly flow over the North Atlantic main development region and enhances the climatological wind shear pattern, which is detrimental to cyclogenesis in the North Atlantic (Gray 1984; Wu and Lau 1992). This is similar to the reduction of tropical storms in the North Atlantic region in WARM, which we have shown is due to increases in upper level westerly flow and vertical wind shear (Fig. 10c). The mechanisms that occur in WARM and El Niño are also similar in the Northwest Pacific. In this region most tropical storms form in the monsoon trough and during El Niño years the monsoon trough develops an anomalous eastward extension in the Northwest Pacific (see Lander 1994; Harrison 1987). This leads to an eastward shift in the cyclogenesis region and a reduction in the number of tropical storms in the Northwest Pacific during El Niño years. There is then a seesaw in the frequency of tropical storms in the western and central Pacific between La Niña and El Niño years (e.g. Chan 1985; Wu and Lau 1992). As in the observations, N144 has a reduction in the total number of tropical storms and an eastward shift in genesis in El Niño years (Fig. 11). These are similar to the changes which occur in WARM (Fig. 9c). There is also an extension of the monsoon trough in WARM (Fig. 10b) and more tropical storms form where it has extended (Fig. 9c).

In summary, the changes in SSTs do not always directly drive the changes in tropical storms in WARM as the SSTs increase in all regions, but there are both increases and decreases in tropical storms. However, in the North Atlantic and Northwest Pacific regions the SST response is like the El Niño response and in this instance the SST changes are likely to be responsible for the main signal in the tropical storm response.

7 Diagnosing tropical storms in low-resolution models

Long climate change experiments are typically carried out with coupled ocean-atmosphere models with an N48 resolution (e.g. HadCM3 Gordon et al. 2000) or something similar, due to the limitations imposed by computing resources. Here, we test whether any useful information about changes in tropical storms can be diagnosed from these experiments.

Table 3 Annual mean number of tropical storms per year calculated using ConvGP in the tropics, Northern Hemisphere and Southern Hemisphere for N144, N48, WARM (15-year mean), WARM minus N144 and GHG minus CON

	Tropics 30°S–30°N	Northern Hemisphere 0–30°N	Southern Hemisphere 0–30°S
OBS	82	58	25
N144	86	45 (0.45)	41 (0.54)
N48	80	43 (0.07)	37 (0.49)
WARM	93	52	41
WARM-N144	7 (8%)	7 (16%)	0
GHG-CON	1 (1%)	5 (12%)	−4 (9%)

The correlations of the number of storms in each season for the Northern and Southern Hemispheres are shown in parenthesis for OBS and N144 and for OBS and N48. Absolute correlations greater than 0.54 (0.56) are significant at the 5% level using a two-sided test for the Northern Hemisphere (for the Southern Hemisphere). The season is from December to November (of following year) in the Northern Hemisphere and from July to June (of the following year) for the Southern Hemisphere, giving 17 years of data in the Northern Hemisphere and 16 years of data in the Southern Hemisphere. The percentage change from N144 to WARM and CON (20-year mean) to GHG (2080–2100 mean) are also given in parenthesis. The OBS results as on Table 1 are provided for comparison

7.1 Can TRACKS be usefully applied to models with low horizontal resolution?

The structure of an example of a tropical storm from N48 shows that tropical storms are not as well simulated by N48 as by N144 (Fig. 1). In comparison to the observed tropical storm the winds are too weak and the radius is too large (approximately two times too large in the example shown) due to the coarse, simplified structure of the tropical storm. In addition, N48 does not capture horizontally small tropical storms and both the initial disturbances and tropical storms are large relative to those in N144. Therefore the tropical storms that are picked up by TRACKS tend to be larger and weaker than the tropical storms in N144. For these reasons and possibly other reasons such as the resolution dependency of the physical parameterizations in the model, TS genesis is lower in all basins than in observations (compare Figs. 12a to 2a). In particular the Northeast Pacific (Fig. 4c) and North Atlantic (Fig. 4d) basins have virtually no cyclogenesis and the Southwest Indian (Fig. 4e) and Southwest Pacific (Fig. 4f) basins have very little TS activity. Only the North Indian (Fig. 4a) and Northwest Pacific (Fig. 4b) basins produce numbers of TSs that are similar to those observed. This could be because large-scale features of the circulation drive a large proportion of the model TSs in these regions. In the North Indian basin (Fig. 4b), the annual cycle, as in N144, consists of only one peak period rather than the observed two peaks.

7.2 Are the results of the ConvGP resolution-dependent?

Compared to TRACKS, the ConvGP for N48 yields more tropical storms (Fig. 12) and the annual cycles in each basin (not shown) agree well with those of the N144 ConvGP. For this comparison, the value of k ($k = 0.125$) used to calculate the ConvGP for N48 was chosen so that the global cyclogenesis frequency predicted by the ConvGP equalled the global cyclogenesis frequency according to the ConvGP in N144. This constraint effectively limited the effects of resolution differences between N144 and N48 to changes in their annual cycles and spatial distribution in each basin, while preserving the global mean number of tropical storms in each experiment as approximately equal to that observed (see Table 3). As with N144 TRACKS and ConvGP, the correlations between OBS and N48 are not significant (Table 3). It is important to note that the ConvGP gives a good regional diagnosis of tropical storms with the caveat that the global number of tropical storms is constrained.

The genesis of tropical storms in N48, as diagnosed by both TRACKS and the ConvGP, shows that N48 has the mean (large-scale) conditions to produce tropical storms, but is unable to resolve the individual tracks as well as N144. The latter point confirms the results of

Table 4 Mean number of tropical storms per season in the Northeast Pacific and North Atlantic ocean basins for OBS (17-year mean), N144 (17-year mean), WARM (15-year mean), WARM minus N144, and percentage change from N144 to WARM

	Northeast Pacific				North Atlantic			
	DJF	MAM	JJA	SON	DJF	MAM	JJA	SON
OBS	0.2	0.7	11.1	7.1	0.0	0.1	3.6	4.2
TRACKS								
N144	0.3	0.4	4.8	4.7	0.4	0.7	2.4	4.8
WARM	1.1	0.5	6.9	9.7	0.5	0.9	1.2	3.1
WARM-N144	0.8	0.1	2.1	5.0	0.1	0.2	−1.2	−1.7
%change (%)	267	20	44	106	25	29	−50	−35
GrayGP								
N144	0.2	0.7	2.1	0.5	0.1	0.1	1.4	1.2
WARM	1.7	3.8	10.0	9.2	0.3	1.0	3.8	2.5
WARM-N144	1.5	3.1	7.9	8.7	0.2	0.9	2.4	1.3
%change (%)	750	443	376	1,750	414	900	171	108
ConvGP								
N144	0.7	0.9	3.1	2.7	0.4	0.5	2.4	2.1
WARM	1.0	1.2	3.4	4.3	0.3	0.5	1.8	1.6
WARM-N144	0.3	0.3	0.3	1.6	−0.1	0.0	−0.6	−0.5
%change (%)	43	33	10	59	25	0	−25	24

The model results are calculated using TRACKS, GrayGP and ConvGP

Bengtsson et al. (1995), who proposed that the representation of tropical storms would be improved as model resolution is increased. Lighthill et al. (1994) argued that GCMs could not be used to study tropical storms. However, in recent years the complexity and resolution of climate models has progressed to a level where, as we have shown, this statement is no longer true for many models.

The ConvGP gives a good indication of where tropical storms should be in N48; whereas, TRACKS does not, because of the poor simulation of individual tropical storms by N48. In general, the results of the ConvGP are independent of whether N144 or N48 data is used because it diagnoses tropical storm genesis from the large-scale conditions which are well simulated by both models.

7.3 Can the genesis parameters give useful information on changes in TSs in climate-change simulations?

If changes in tropical storms are determined mostly by changes in the large-scale forcing, then N48 may give a reasonable indication of changes in tropical storms in a climate change scenario. We apply the ConvGP to data from the HadCM3 coupled model that has an atmospheric resolution of N48. We use data for the period 2080 to 2100 for the control experiment (CON) and IS95a greenhouse gas experiment (GHG). These are the experiments that were used to create the SST forcing fields for WARM. The change in SST, is therefore, essentially the same as the difference between WARM and N144, except for natural variability. Overall, the CON ConvGP (not shown) produces the same pattern of TS genesis as the N144 ConvGP, but the maxima regions have fewer tropical storms and are slightly displaced compared to N144. The ConvGP difference of GHG minus CON (Fig. 13a) is very similar to WARM minus N144 (Fig. 9c), despite the differences in the control simulations. Again, there is less detail available in the maxima regions than in N144. However, the changes in GHG are, in many areas, not as large as the changes in WARM. The changes in the Northern Hemisphere are similar to those in WARM, but, unlike in WARM, there are fewer tropical storms in GHG than in CON in the Southern Hemisphere (Table 3). The similarities between GHG minus CON and WARM minus N144 in the ConvGP suggest that the ConvGP response is fairly robust to the change in resolution. The qualitative similarity between ConvGP and tracks for WARM minus N144 suggests that the tropical storms are responding to changes in the large-scale forcing.

As an additional test of the ConvGP, we analyse the changes due to ENSO in CON. The advantage of using this experiment instead of N144 is that there is more data available. Here, we calculate the El Niño and La Niña ConvGP composites for 100 years of CON in the same way as for N144. There are 27 El Niño years and 26 La Niña years in this sample. As with the high-resolution experiments, the difference between the coupled model El Niño and La Niña composites (Fig. 13b) is similar to the climate change pattern in the ConvGP in some regions (Fig. 13a).

The similarity of the HadCM3 response to the high-resolution experiment response in both the climate change experiments and in the ENSO changes suggests that the ConvGP may give an indication of the re-

▶

Fig. 10 Annual mean differences of WARM (15-year mean) minus N144 (17-year mean). **a** Sea surface temperature with a shading interval of 1 K. *Bold solid line* is 26.5°C isotherm from WARM and *bold dashed line* is 26.5°C isotherm from N144. **b** Relative vorticity on 850 hPa, with a shading interval of 1.0×10^{-6} s^{-1}. Cyclonic relative vorticity is positive in the Northern Hemisphere and negative in the Southern Hemisphere. The contours show velocity potential on 850 hPa. **Dashed line** is -0.75×10^{6} m^2 s^{-1}, *dotted line* is zero and *solid line* is 0.75×10^{6} m^2 s^{-1}. Divergent winds point from negative to positive velocity potential and are proportional to the gradient of the velocity potential. **c** Vertical shear of horizontal wind between 925 and 200 hPa, with a shading interval of 2.0 ms^{-1} per 725 hPa. **d** Convective rainfall rate with a shading interval of 1 mm day^{-1}, increases are shown in *blue* on Fig. 10d sponse of tropical storms in lower resolution model simulations of climate change. Also, as the tropical storms respond to the large-scale flow, it may not be necessary to actually resolve them to get estimates of how they may change under global warming conditions. This means that ensembles of longer climate

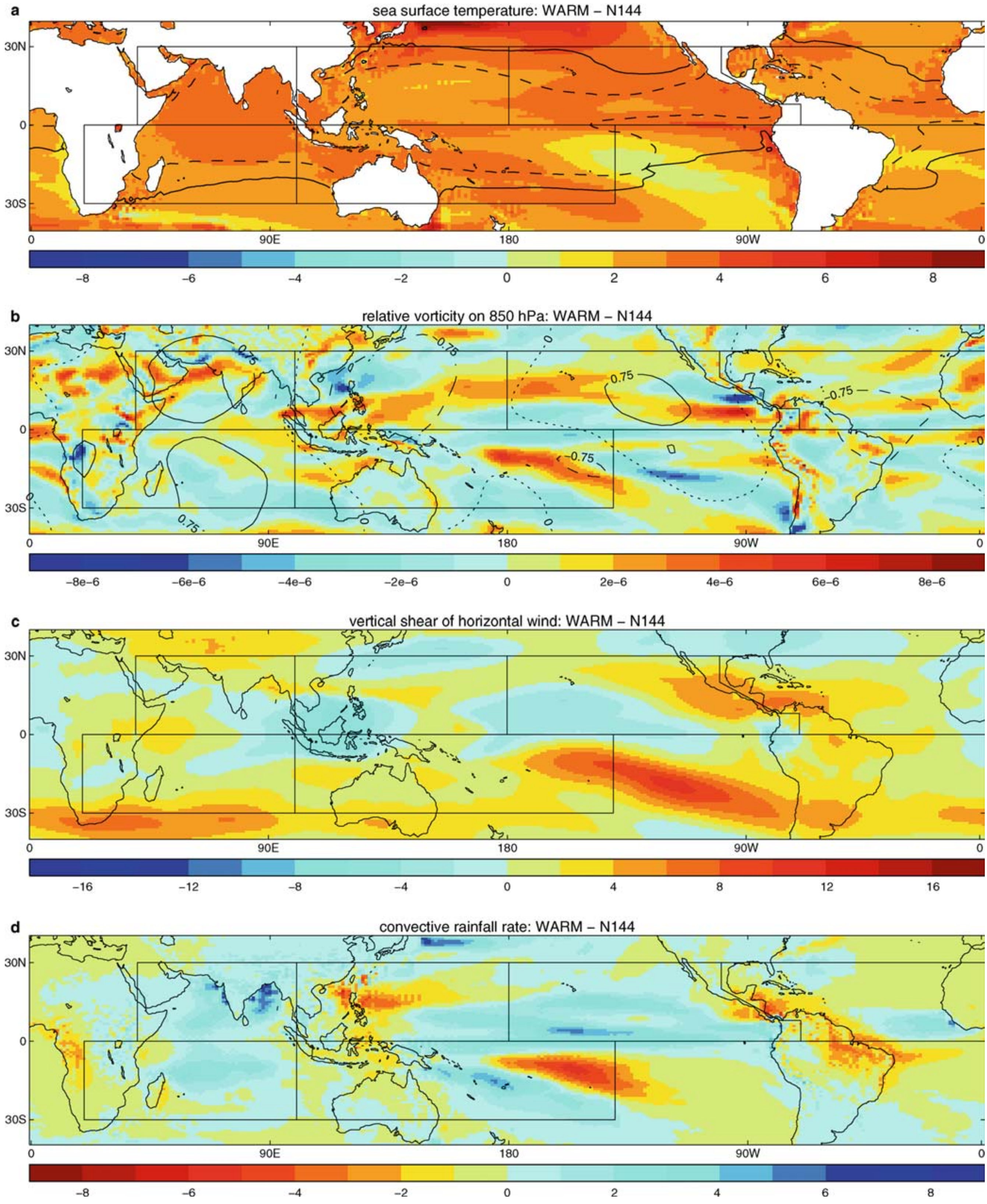

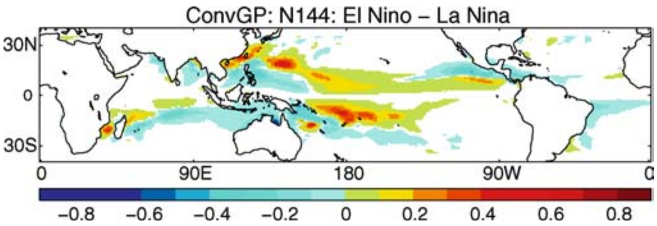

Fig. 11 Density of tropical storm genesis as diagnosed by the ConvGP for the composite of 6 El Niño years minus the composite of 4 La Niña years from 17 years of N144 data. The shading interval is 0.1 tropical storms per 1° latitude×1° longitude area per 17 year

change experiments, which are usually carried out with models of the same resolution as HadCM3, can give some useful information about changes in tropical storm genesis, without actually resolving the tropical storms. The use of long experiments and ensembles of experiments increases the statistical significance and reduced the uncertainties of the results. However, the information provided by the ConvGP is limited. For more detail about tropical storms it is necessary to use a model which can resolve them, so that a technique like TRACKS can be applied.

8 Conclusions

The three main questions that we aim to answer in this study are:

1. How well does the high-resolution model simulate tropical storms?
2. What are the changes in tropical storms under global warming conditions?
3. Can any useful information about tropical storms be gained from experiments carried out with low-resolution models using either TRACKS or the genesis parameters?

To answer the first question, we analyse tropical storm tracks in an atmosphere only model that has a high horizontal resolution (N144–0.83° latitude by 1.25° longitude) and is forced with observed SSTs and sea ice. The model grid-scale is larger than the typical scale of the intense inner core of observed tropical cyclones, but it is able to simulate TS-like features. In most regions, the distribution and annual cycles of the simulated tropical storms compare well with observations. However, globally there are too many tropical storms and the distribution has errors common to many models. We feel that despite the errors in the simulation of tropical storms in N144, this model is a useful tool for exploring the mechanisms of the response of tropical storms to climate change, particularly as there is some evidence that realistic physical mechanisms are producing tropical storms.

To answer the second question, we carry out a global warming experiment (WARM) and this produces 6% fewer tropical storms globally, but there are large regional variations in the sign of the changes. Using TRACKS, we find that in our model there are more tropical storms in the Northeast Pacific, North Indian and South Indian Ocean basins and fewer tropical storms in the North Atlantic, Northwest Pacific and Southwest Pacific ocean basins. Maximum cyclogenesis shifts away from the coasts in the Northwest Pacific, Northeast Pacific and Southwest Indian regions and shifts southward in the Southwest Pacific region. Most of the changes occur in the peak seasons with little change in timings. There is evidence of a slight increase in tropical storm intensity under climate change conditions.

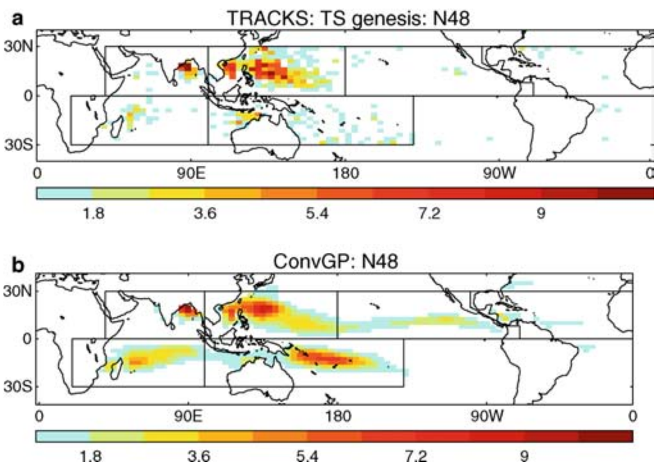

Fig. 12 **a** Density of TS genesis, as diagnosed by TRACKS, for N48 (17 years, 1 December 1978 to 1 December 1995). The field has been nine point area averaged. **b** Density of tropical storm genesis, as diagnosed by the ConvGP, for N48 (17-year mean). The shading interval is 0.9 tropical storms per 2.5° latitude×3.75° longitude area per 17 year. This is 9× the scale used in both Figs. 2b and 9b, as the resolution of N144 is 9× the resolution of N48

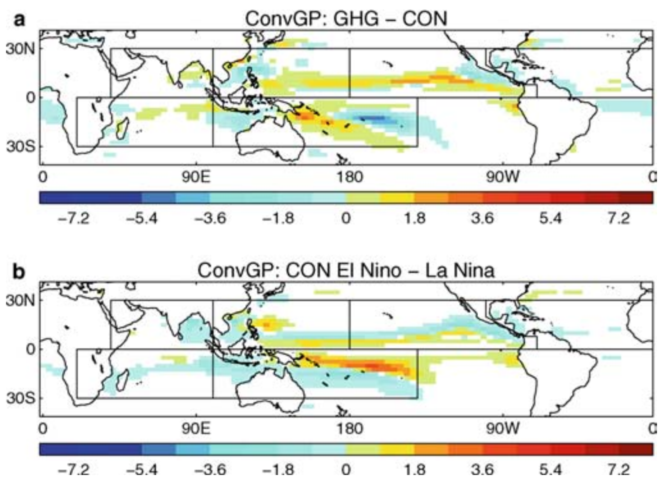

Fig. 13 Density of tropical storm genesis as diagnosed by the ConvGP. The shading interval is 0.9 tropical storms per 2.5° latitude × 3.75° longitude area per 17 year. **a** GHG (2080–2100) minus CON (20 year). **b** Composite of El Niño 26 years minus composite of La Niña 27 years based on 100 year of CON data

The changes in SSTs do not always directly drive the changes in tropical storms in WARM. SSTs increase in all regions, but some regions have fewer tropical storms. The changes in tropical storms are consistent with the changes in the background large-scale atmospheric circulation, with more tropical storms forming where the low-level flow is more cyclonic and convergent. In most regions, there are more TSs where there is more convective rainfall.

El Niño produces a characteristic response in tropical storms that is well represented in our model in the N144 integration. The SST response under climate change (WARM) has similarities to El Niño in some regions, in particular, the North Atlantic and Northwest Pacific. The relevant large-scale circulation response and consequent tropical storm response is also similar.

To answer the final question, we first carry out a present day simulation with a standard resolution model (N48). This produces less realistic and weaker tropical storms than in N144, confirming that the number, structure and intensity of individual tropical storms improve as model resolution is increased. Indeed, the model does not capture enough individual storms for the tracking technique to be viable. By applying the TS genesis parameters to the low- and high-resolution model runs in present and future climates, we are able to demonstrate that the low-resolution model captures the important current and future large-scale structure present in the high-resolution runs. Hence, the genesis parameters can be used as a proxy for tropical storms in low-resolution simulations of current and possible future climate.

The choice of parameter is important, however. While the original Gray's genesis parameter (GrayGP) works well for current climate, it predicts far too many storms in future climate as it is dominated by the changes in SSTs. The newer convective genesis parameter (ConvGP), on the other hand, works well in both current and future climate simulations. Assuming these results can be generalised to other models, ConvGP could be used to diagnose changes in tropical storms in long climate change experiments, which are usually carried out at lower horizontal and vertical resolutions. This is important, because the short time-slice experiments used here do not capture the full range of natural variability or uncertainty in the climate system and models of it. Physics and initial condition ensembles and long integrations are needed to quantify these effects, and for these lower resolution models are needed.

We conclude that whilst the simulation of tropical storms is improved in higher resolution models, there is useful information about tropical storm genesis and the relevant background conditions in low-resolution models. However, for more detailed information about TS life cycles, and in particular storm intensity, high-resolution experiments are necessary.

Acknowledgements This work was carried out under the UK Government Meteorological Research Programme. Rachel Stratton carried out the N144 and N48 experiments and Tim Johns carried out the HadCM3 experiments. Kevin Hodges of Reading University wrote the tracking programs and David Jackson modified the tracking to identify TSs. We would like to thank the anonymous reviewers for their detailed comments that have improved this paper. We thank ECMWF for the use of their reanalysis (ERA) dataset and the CPC for the use of the CMAP data. We also thank the Joint Typhoon Warning Center (JTWC), Colorado State University and the Tropical Prediction Center for the use of their tropical storm best track data. The Southern Hemisphere and North Indian data were downloaded from http://metoc.npmoc.navy.mil/jtwc/best_tracks/ and the Northwest Pacific, North Atlantic, and Northeast Pacific data were downloaded from http://weather.unisys.com/hurricane/.

Appendix The tracking technique (TRACKS)

We locate and track tropical storms by applying a two stage objective technique to data at 12-h intervals. In the first stage (Hodges 1994), we track local centres of 850 hPa relative vorticity with a magnitude greater than 5×10^{-5} s^{-1}. We track relative vorticity centres on 850 hPa as this is a more effective way of identifying tropical storm tracks than by tracking centres of low pressure (Serrano 1997). We selected the threshold of 5×10^{-5} s^{-1} after carrying out some simple tests using the N144 experiment.

However, even with our chosen threshold, the relative vorticity tracks still include some systems which are not TSs and so in the second stage we filter the tracks to select only TSs. As well as satisfying strength, lifetime and formation region criteria each track has to have a warm core. The warm core conditions are applied to temperature anomalies (T_a), which are defined as the temperature at the centre minus the mean temperature of a 15° by 15° region surrounding the centre.

In summary, the criteria that we used to identify tropical storms are:

A local maximum of 850 hPa relative vorticity with an absolute value greater than 5.0×10^{-5} s^{-1} at all points along the track.

The tropical storm forms over the ocean between the latitudes of 30°N and 30°S.

The lifetime of the tropical storm is at least 2 days.

T_a on 300 hPa $>$ 0.0, at all points along the track.

T_a on 300 hPa $>$ 0.5 K, for any two of the first, middle or last points of the track.

T_a on 300 hPa $>$ T_a on 850 hPa, for any two of the first, middle or last points of the track.

In N48 the temperature anomalies on 300 hPa were replaced by anomalies on 200 hPa, as temperature data on 300 hPa was not available for this experiment.

References

Bengtsson L, Botzet M, Esch M (1995) Hurricane-type vortices in a general circulation model. Tellus 47A:175–196

Bengtsson L, Botzet M, Esch M (1996) Will greenhouse gas-induced warming over the next 50 years lead to a higher frequency and greater intensity of hurricanes? Tellus 48A:57–73

Chan JCL (1985) Tropical cyclone activity in the Northwest Pacific in relation to the El Niño/Southern Oscillation phenomenon. Mon Weather Rev 113:599–606

Cubasch U, Meehl GA, Boer GJ, Stouffer RJ, Dix M, Noda A, Senior CA, Rapa S, Yap KS (2001) Projections of future climate change. In: Houghton JT, Ding Y, Griggs DJ, Noguer M, van der Linden PJ, Dai X, Maskell K, Johnson CA (eds) Climate change 2001: the scientific basis. Contribution of working group I to the third assessment report of the intergovernmental panel on climate change. Cambridge University Press, Cambridge, p 881

Cullen MJP (1993) The unified forecast/climate model. Meteorol Mag 122:81–94

Davis MAS, Brown GM, Leftwich P (1984) A tropical cyclone data tape for the Eastern and Central North Pacific Basins, 1949–1983: contents, limitations, and uses. NOAA Tech Memorandum NWS NHC 25

Emanuel KA (1987) The dependence of hurricane intensity on climate. Nature 326:483–485

Gibson R, Kållberg P, Uppala S, Hernandez A, Normura A and Serrano E (1997) ERA description, re-analysis (ERA) project report series 1. ECMWF, Shinfield Park

Giorgi F, Hewitson B, Christensen J, Hulme M, Von Storch H, Whetton P, Jones R, Mearns L, Fu C (2001) Regional climate information—evaluation and projections. In: Houghton JT, Ding Y, Griggs DJ, Noguer M, van der Linden PJ, Dai X, Maskell K, Johnson CA Climate change 2001: the scientific basis. Contribution of working group I to the third assessment report of the intergovernmental panel on climate change. Cambridge University Press, Cambridge

Gordon C, Cooper C, Senior CA, Banks H, Gregory JM, Johns TC, Mitchell JFB, Woods RA (2000) The simulation of SST, sea-ice extents and ocean heat transports in a version of the Hadley Centre coupled model without flux adjustments. Climate Dynam 16:147–168

Gray WM (1968) Global view of the origin of tropical disturbances and storms. Mon Weather Rev 96:669–700

Gray WM (1979) Hurricanes: their formation, structure and likely role in the tropical circulation. In: Shaw DB (ed) Meteorology over the Tropical Oceans. Royal Meteor Soc 155–218

Gray WM (1984) Atlantic seasonal hurricane frequency. Part I: El Niño and 30 mb quasi-biennial oscillation influences. Mon Weather Rev 112:1649–1668

Haarsma RJ, Mitchell JFB, Senior CA (1993) Tropical disturbances in a GCM. Climate Dynam 8:247–257

Harrison DE (1987) Monthly mean island surface winds in the central tropical Pacific and El Niño events. Mon Weather Rev 115:3133–3145

Henderson-Sellers A, Zhang H, Berz G, Emanuel K, Gray W, Landsea C, Holland G, Lighthill J, Shieh S-L, Webster P, McGuffe K (1998) Tropical cyclones and global climate change: a post-IPCC assessment. Bull Amer Meteorol Soc 79:19–38

Hodges KI (1994) A general method for tracking analysis and its application to meteorological data. Mon Weather Rev 122:2573–2586

Holland GJ (1997) The maximum potential intensity of tropical cyclones. J Atmos Sci 54:2519–2541

Houghton JT, Meira Filho LG, Callander BA, Harris N, Kattenberg A, Maskell K (1996) Climate change 1995: the science of climate change. contribution of working group I to the second assessment report of the intergovernmental panel on climate change. Cambridge University Press, Cambridge

Jarvinen BR, Neumann CJ, Davis MAS (1984) A tropical cyclone data tape for the North Atlantic Basin, 1886–1983: contents, limitations, and uses. NOAA Tech Memorandum NWS NHC 22

Kållberg P (1998) Aspects of the re-analysed climate. Re-analysis (ERA) project report series 2, ECMWF, Shinfield Park

Knutson TR, Tuleya RE (1999) Increased hurricane intensities with CO_2 induced warming as simulated using the GFDL hurricane prediction system. Climate Dynam 15:503–519

Lander MA (1994) An exploratory analysis of the relationship between tropical storm formation in the western North Pacific and ENSO. Mon Weather Rev 122:636–651

Landsea CW (1993) A climatology of intense (or major) Atlantic hurricanes. Mon Weather Rev 121:1703–1713

Lighthill J, Holland G, Gray W, Landsea C, Craig G, Evans J, Kurihara Y, Guard C (1994) Global climate change and tropical cyclones. Bull Amer Meteorol Soc 75:2147–2157

Palmen E (1948) On the formation and structure of tropical hurricanes. Geophysica 3:26–38

Philander SG (1990) El Niño, La Niña and the Southern Oscillation. International Geophysics Series, vol 46. Academic Press, New York, p 293

Pope VD, Stratton RA (2002) The processes governing resolution-sensitivity in a climate model. Climate Dynam 19:211–236

Pope VD, Gallani ML, Rowntree PR, Stratton RA (2000) The impact of new physical parametrizations in the Hadley Centre climate model—HadAM3. Climate Dynam 16:123–146

Royer J-F, Chauvin F, Timbal B, Araspin P and Grimal D (1998) A GCM study of the impact of greenhouse gas increase on the frequency of occurrence of tropical cyclones. Clim Change 38:307–343

Ryan BF, Watterson IG, Evans JL (1992) Tropical cyclones frequencies inferred from Gray's yearly genesis parameter: validation of GCM tropical climate. Geophys Res Lett 19:1831–1834

Serrano E (1997) Tropical cyclones. ECMWF re-analysis project report series 5, ECMWF

Sugi M, Noda A, Sato N (2002) Influence of global warming on tropical cyclone climatology: an experiment with the JMA global model. J Meteorol Soc Jpn 80:249–272

Vitart F, Anderson LJ, Stern WF (1997) Simulation of inter-annual variability of tropical storm frequency in an ensemble of GCM integrations. J Clim 10:745–760

Walsh KJE (1997) Objective detection of tropical cyclones in high-resolution analyses. Mon Weather Rev 125:1767–1779

Walsh KJE, Ryan BF (2000) Tropical cyclone intensity increase near Australia as a result of climate change. J Clim 13:3029–3036

Walsh KJE, Watterson IG (1997) Tropical cyclone-like vortices in a limited area model: comparison with observed climatology. J Clim 10:2240–2259

Watterson IG, Evans JL, Ryan BF (1995) Seasonal and inter-annual variability of tropical cyclogenesis: diagnostics from large-scale fields. J Clim 8:3052–3066

Williams KD, Senior CA, Mitchell JFB (2001) Transient climate change in the Hadley Centre models: the role of physical processes. J Clim 14:2659–2674

Wu G, Lau N-C (1992) A GCM simulation of the relationship between tropical storm formation and ENSO. Mon Weather Rev 120:958–977

Xie P, Arkin PA (1997) Global precipitation: a 17-year monthly analysis based on gauge observations, satellite estimates and numerical model outputs. Bull Amer Meteorol Soc 78:2539–2558